
ES-ENAS: Controller-Based Architecture Search for Evolutionary Reinforcement Learning

Xingyou Song^{*1}, Krzysztof Choromanski^{1,2}, Jack Parker-Holder³, Yunhao Tang²,
 Daiyi Peng¹, Deepali Jain¹, Wenbo Gao⁴, Aldo Pacchiano⁵, Tamas Sarlos¹, Yuxiang Yang⁶
¹Google, ²Columbia U., ³Oxford U., ⁴Waymo, ⁵UC Berkeley, ⁶U. of Washington

Abstract

We introduce ES-ENAS, a simple yet general evolutionary joint optimization procedure by combining continuous optimization via Evolutionary Strategies (ES) [38, 29] and combinatorial optimization via Efficient NAS (ENAS) [50, 34, 54] in a highly scalable and intuitive way. Our main insight is noticing that ES is already a highly distributed algorithm involving hundreds of forward passes which can not only be used for training neural network weights, but also for jointly training a NAS controller, both in a blackbox fashion. By doing so, we also bridge the gap from NAS research in supervised learning settings to the reinforcement learning scenario through this relatively simple marriage between two different yet common lines of research. We demonstrate the utility and effectiveness of our method over a large search space by training highly combinatorial neural network architectures for RL problems in continuous control, via edge pruning and quantization. We also incorporate a wide variety of popular techniques from modern NAS literature including multiobjective optimization along with various controller methods, to showcase their promise in the RL field and discuss possible extensions.

1 Introduction

Neural network architectures are the basic building blocks of modern deep learning, as they determine the inductive biases that models will use to process information and make predictions. Normally, these building blocks are hand-designed using human intuition and priors, such as convolutional layers which are based on the principle of visual locality. Unfortunately, finding the right architecture using e.g. the best possible combination of convolutions, can sometimes be a very tedious and laborious task, which requires training multiple models iteratively. Neural architecture search (NAS) [54], however, seeks to automate this process to both reduce human labor as well as find optimal architectures that humans may overlook. NAS has been successfully applied to designing model architectures in fields ranging from image classification [54] to language modeling [41], and has even been applied to algorithm search [36]. However, surprisingly, one field which has *not* seen relative popularity with standard NAS techniques is *reinforcement learning* (RL).

While some variants of NAS specifically mix in the optimization process with the model, for example Differentiable Architecture Search (DARTS) [27], in many cases, the objective is treated as a blackbox function $f : \mathcal{M} \rightarrow \mathbb{R}$ where \mathcal{M} is a combinatorial, discrete search space representing potential components of a model architecture, and the objective is the accuracy of the model once trained to convergence. This blackbox framework is exploited in the original NAS paper [54], where a central *controller*, first introduced as a RNN-based Pointer Network [50], parameterizes the search space \mathcal{M} with a distribution p_ϕ via neural network parameters ϕ , and proposes candidate architectures, i.e. *child models* $m \in \mathcal{M}$ to obtain objectives from which to train ϕ via policy gradient.

*Correspondence to xingyousong@google.com.

Code: github.com/google-research/google-research/tree/master/es_enas

Coincidentally, the blackbox framework has been used in RL as well. One such rather conceptually simple RL algorithm is Evolutionary Strategies (ES) [38], also known as Augmented Random Search (ARS) [29, 30], which estimates a Gaussian smoothed gradient of the objective, by using multiple CPU workers for forward pass evaluation. ES sidesteps notions of replay buffers and simply treats an agent’s total reward as a blackbox (and potentially non-differentiable) objective $f(\theta)$ in terms of θ , the agent’s neural network parameters. This allows more flexible classes of combinatorial and non-differentiable policies to be used as well. ES has been applied successfully to multiple domains such as Atari and especially in robotics due to its ability to train stable deterministic policies in continuous control tasks.

What follows on how to combine NAS with ES should therefore be intuitive, as they are both *blackbox algorithms* and use very similar distributed workflows. Our key observation is that **one can simply introduce a NAS controller into the central aggregator in ES in a highly scalable but conceptually straightforward way**. This leverages the large population, on the order of hundreds to thousands, of cheap CPU workers for blackbox evaluations $f(m, \theta)$ that jointly optimize the controller supplying models m and neural network weights θ . In doing so, we are one of the first to apply popular controller-based NAS techniques to the field of RL. A visual representation of our algorithm can be found in Fig. 1.

We thus introduce the ES-ENAS algorithm, which requires no extra computational resources and empirically demonstrate its utility on large combinatorial search spaces for neural network edge pruning and quantization.

2 ES-ENAS Method

2.1 Preliminaries

In the standard RL setting, consider a Markov Decision Process (MDP), or environment \mathcal{E} with state space $\mathcal{S} \subseteq \mathbb{R}^{|\mathcal{S}|}$ and action space $\mathcal{A} \subseteq \mathbb{R}^{|\mathcal{A}|}$ and an agent aiming to maximize its total expected/discounted reward obtained from interacting in \mathcal{E} . In deep reinforcement learning, the standard approach is to construct a neural network policy $\pi_\theta(s) = a$ which maps states $s \in \mathcal{S}$ to actions $a \in \mathcal{A}$, and is parameterized by θ , the neural network’s weights. The blackbox objective is to maximize the sum of rewards $f(\theta) = \sum_{t=1}^T r_t$ obtained in the environment from a given trajectory of states and actions $(s_1, a_1, s_2, a_2, \dots, s_T, a_T)$.

The foundation of our algorithm for learning policy network structure is the class of weight-sharing methods [34], optimized using controller-based methods [54]. Weight sharing builds a maximal *supernet* containing all possible weights θ_s where each *child model* m only utilizes certain subcomponents and their corresponding weights from this supernet. Child models are sampled from a *controller* p_ϕ , where ϕ denotes the current state of the controller. The core idea is to perform

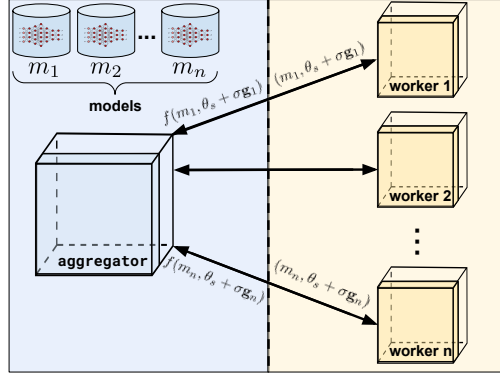


Figure 1: Figure representing our aggregator-worker pipeline, where the aggregator proposes models m_i in addition to a perturbed input $\theta_s + \sigma \mathbf{g}_i$, and the worker the computes the objective $f(m_i, \theta_s + \sigma \mathbf{g}_i)$, which is sent back to the aggregator. Both the training of the weights θ_s and of the model-proposing controller p_ϕ rely on the number of worker samples to improve performance.

Algorithm 1: ES-ENAS Algorithm, with the few additional modifications to allow ENAS shown in blue.

Data: Initial weights θ_s , weight step size η_w , precision parameter σ , number of perturbations n , controller p_ϕ .

```

while not done do
  Sample i.i.d. vectors
   $\mathbf{g}_1, \dots, \mathbf{g}_n \sim \mathcal{N}(0, \mathbf{I})$ ;
  foreach  $\mathbf{g}_i$  do
    Sample  $m_i^+, m_i^- \sim p_\phi$ 
     $v_i^+ \leftarrow f(m_i^+, \theta_s + \sigma \mathbf{g}_i)$ 
     $v_i^- \leftarrow f(m_i^-, \theta_s - \sigma \mathbf{g}_i)$ 
     $v_i \leftarrow \frac{1}{2}(v_i^+ - v_i^-)$ 
     $p_\phi \leftarrow \{(m_i^+, v_i^+), (m_i^-, v_i^-)\}$ 
  end
  Update weights
   $\theta_s \leftarrow \theta_s + \eta_w \frac{1}{\sigma n} \sum_{i=1}^n v_i \mathbf{g}_i$ 
  Update controller  $p_\phi$ 
end

```

alternating updates between θ_s and ϕ in order to respectively, improve both neural network weights and architecture selection at the same time.

We concisely summarize our method in Algorithm 1. Below, we provide its derivation and conceptual simplicity of combining the updates for θ_s and ϕ into a joint optimization procedure.

The optimization problem we are interested in is $\max_{m,\theta} f(m,\theta)$, which represents the sum of rewards over the environment by using a policy whose architecture is m , and weights are θ . In order to make this problem tractable, consider instead, optimization on the smoothed objective:

$$\tilde{f}_\sigma(\phi, \theta) = \mathbb{E}_{m \sim p_\phi, \mathbf{g} \sim \mathcal{N}(0, I)} [f(m, \theta + \sigma \mathbf{g})] \quad (1)$$

2.1.1 Updating the Weights

The gradient with respect to θ becomes:

$$\nabla_\theta \tilde{f}_\sigma(\phi, \theta) = \frac{1}{2\sigma} \mathbb{E}_{m \sim p_\phi, \mathbf{g} \sim \mathcal{N}(0, I)} [(f(m, \theta + \sigma \mathbf{g}) - f(m, \theta - \sigma \mathbf{g})) \mathbf{g}] \quad (2)$$

Note that by linearity, we may move the expectation $\mathbb{E}_{m \sim p_\phi}$ inside into the two terms $f(m, \theta + \sigma \mathbf{g})$ and $f(m, \theta - \sigma \mathbf{g})$, which implies that the gradient expression can be estimated with averaging singleton samples of the form:

$$\frac{1}{2\sigma} (f(m^+, \theta + \sigma \mathbf{g}) - f(m^-, \theta - \sigma \mathbf{g})) \mathbf{g} \quad (3)$$

where m^+, m^- are i.i.d. samples from p_ϕ , and \mathbf{g} from $\mathcal{N}(0, I)$.

Thus we may sample multiple i.i.d. child models $m_1^+, m_1^-, \dots, m_n^+, m_n^- \sim p_\phi$ and also multiple perturbations $\mathbf{g}_1, \dots, \mathbf{g}_n \sim \mathcal{N}(0, I)$ and update the shared weights θ_s with an approximate gradient update:

$$\theta_s \leftarrow \theta_s + \eta_w \left(\frac{1}{n} \sum_{i=1}^n \frac{f(m_i^+, \theta + \sigma \mathbf{g}_i) - f(m_i^-, \theta - \sigma \mathbf{g}_i)}{2\sigma} \mathbf{g}_i \right) \quad (4)$$

This update forms the ‘‘ES’’ portion of ES-ENAS, as inputting a constant fixed model reduces Eq. 4 to standard ES/ARS optimization. Popular CMA-ES [21, 25, 49] and other evolutionary algorithms [51, 22, 24] can also be applied here, although we will show experimentally (Sec 3) that ES is already satisfactory.

2.1.2 Updating the Controller

For the ‘‘ENAS’’ portion of ES-ENAS (i.e. for optimizing the m component), we update p_ϕ by simply reusing the objectives $f(m, \theta + \sigma \mathbf{g})$ already computed for the weight updates. We outline two popular NAS controller methods here: Policy Gradient and Regularized Evolution, which have proven successful for a variety of NAS search spaces, as well as even other applications such as program search [36, 6].

In **Policy Gradient (PG)**, ϕ are the parameters of a RNN-based controller, whose goal is to optimize the smoothed objective $J(\phi) = \mathbb{E}_{m \sim p_\phi} [f(m; \theta_s)]$, whose *policy gradient* can be estimated by:

$$\nabla_\phi J(\phi) = \nabla_\phi \mathbb{E}_{m \sim p_\phi} [f(m, \theta_s)] \approx \frac{1}{n} \sum_{i=1}^n f(m_i, \theta_s) \nabla_{\theta_s} \log p_\phi(m_i) \quad (5)$$

where $\log p_\phi(m)$ is the log-probability of the controller for selecting m , and thus $\phi \leftarrow \phi + \eta_{pg} \nabla_\phi J(\phi)$ is updated with the use of the REINFORCE algorithm [52], or other policy gradient algorithms such as PPO [39].

In **Regularized Evolution (Reg-Evo)** [35], the algorithm state ϕ denotes a population, or *queue* that is first initialized with n models $Q = \{m_1, \dots, m_n\}$ with corresponding scores (slightly abusing notation) $f(Q) = \{f(m_1), \dots, f(m_n)\}$ (or $f(Q, \theta_s)$ ’s instead in the efficient setting). The algorithm then proceeds to construct child models m' via mutating the model $m_{max} = \arg \max_{m \in Q} f(m)$ corresponding to the highest score. These child models are evaluated and appended to Q in a first-in, first-out (FIFO)-like manner, consequently removing the oldest model from Q , otherwise known as *aging evolution*. The authors propose that this addresses the issue of suboptimal models becoming ‘‘stuck’’ in the queue which can be an issue with NEAT [44] and other similar approaches [16, 43].

2.1.3 Setups and Modifications

This mechanism shows that updates to the controller p and updates to the weights θ_s both rely on the samples $f(m, \theta + \sigma \mathbf{g})$. The number of workers n , now serves the two purposes: reducing the sample complexity of the controller p , as well as the variance of the estimated ES gradient $\nabla_{\theta} \tilde{f}_{\sigma}$. ES usually uses many more workers (on the order of 10^2) than what is normal in SL (on the order of 10^0 to 10^1 of workers) which can be important for the controller’s performance, as we will demonstrate in Subsection 3.4.

With the advent of standardized NAS API such as PyGlove [33], search spaces are usually constructed via combinations of primitives involving categorical and conditional parameters. Thus, a child model m can first simply be programmatically represented via Python dictionaries and strings to be sent over a distributed communication channel to a worker alongside the perturbation $\theta + \sigma \mathbf{g}$, and then materialized later by the worker into an actual neural network architecture. Although the controller needs to output hundreds of model suggestions, it can be parallelized to run quickly by multithreading (for Reg-Evo) or by simply using a GPU (for policy gradient).

Furthermore, the controller p_{ϕ} ’s objective can also be defined differently from the weights θ_s ’s objective. This is already subtly the case in supervised learning, where the controller’s objective is the *nondifferentiable validation accuracy* of the model, while the model weights are explicitly optimizing against the *differentiable cross-entropy training loss* of the model. More significant differences between the controller objective and weight objective involve cases such as efficiency and runtime of the network, which have led to work in EfficientNets [47]. We show this can also be applied for the RL setting in Subsection 3.3.

3 Experiments

While the mentioned ES-ENAS algorithm is a general purpose algorithm which allows a multitude of potential applications and modifications, we apply our method to two combinatorial problems, **Sparsification** and **Quantization**, on standard Mujoco [48] benchmarks from OpenAI Gym. These scenarios possess very large combinatorial policy search spaces (calculated as $|\mathcal{M}| > 10^{68}$, comparable to 10^{49} from NASBench [53] - see below for calculations) that will stress test our ES-ENAS algorithm and are also relevant to mobile robotics [14]. A purely random search will clearly be unable to exhaust the entire search space, and will also likely have difficulty attaining high rewards, which we confirm as a sanity check in Subsection 3.2. We first explain our search space definitions:

3.1 Search Space Definitions

In order to allow combinatorial flexibility, our neural network consists of vertices/values $V = \{v_1, \dots, v_k\}$, where the initial block of $|\mathcal{S}|$ values $\{v_1, \dots, v_{|\mathcal{S}|}\}$ corresponds to the environment state, and the last block of $|\mathcal{A}|$ values $\{v_{k-|\mathcal{A}|+1}, \dots, v_k\}$ corresponds to the action output values. Directed edges $E \subseteq E_{max} = \{e_{i,j} = (i,j) \mid |\mathcal{S}| < i < j \leq k\}$ are constructed with corresponding weights $W = \{w_{i,j} \mid (i,j) \in E\}$, and nonlinearities $G = \{\sigma_{|\mathcal{S}|+1}, \dots, \sigma_k\}$ for the non-state vertices. Thus a forward propagation consists of for-looping in order $j \in \{|\mathcal{S}| + 1, \dots, k\}$ and computing output values $v_j = \sigma_j \left(\sum_{(i,j) \in E} v_i w_{i,j} \right)$.

We can easily build search spaces using *primitives* in PyGlove [33], such as “pyglove.oneof” and “pyglove.manyof” operations, which respectively choose one item, or a combination of multiple objects from a container. These primitives can be combined in a nested structure via “pyglove.List” or “pyglove.Dict”. The search space can then be sent to a pre-implemented controller (such is the case for Reg-Evo, Policy Gradient, and pure random search), which proposes instances from the space.

3.1.1 Edge Pruning

Sparsification and edge-pruning follows a long history with methods such as [37, 3, 31] from the 1980’s, Optimal Brain Damage [9], regularization [28], magnitude-based weight pruning methods [20, 40, 32], sparse network learning [18, 26], and discoveries such as the Lottery Ticket Hypothesis [13]. These works often manage to match the performance of original networks with up to 90%

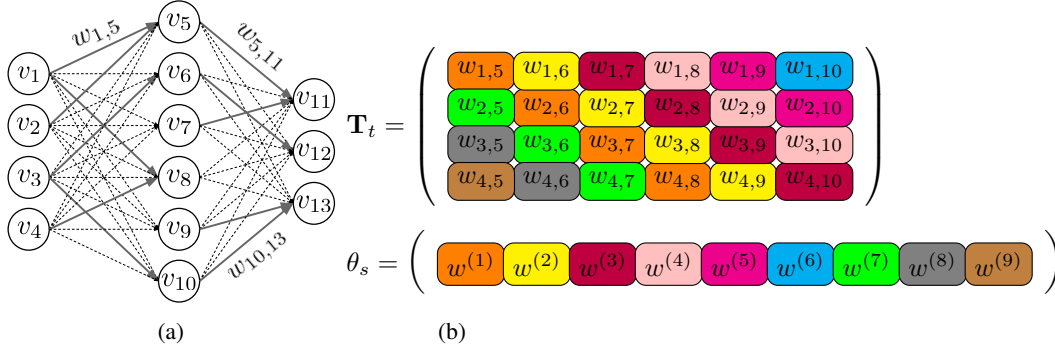


Figure 2: (a) Example of our neural network setup with selected edges and corresponding weight labels, when $|\mathcal{S}| = 4$ and $|\mathcal{A}| = 3$, with a hidden layer of size 6. Solid edges are those learned by the algorithm. (b) Example of quantization mechanism using a Toeplitz pattern [5], for the first layer in Fig. 2a. Entries in each of the diagonals are colored the same, thus sharing the same weight value. The trainable weights $\theta_s = (w^{(1)}, \dots, w^{(9)})$ are denoted at the very bottom in the vectorized form. As we see, a weight matrix with 24 entries is effectively encoded by a 9-dimensional vector.

fewer parameters on classification tasks. We ultimately confirm these findings in the RL setting by showing that good rewards can be obtained up to a high level of pruning.

Thus, for our **edge pruning** method, we group all possible edges (i, j) into a set in the neural network, and select a fixed number of edges from this set. We can also further search across potentially different nonlinearities, e.g. $f_i \in \{\tanh, \text{sigmoid}, \sin, \dots\}$ similarly to Weight Agnostic Neural Networks [15]. In terms of API, this search space can be described as `pyglove.manyof($E_{max}, |E|$)` along with `pyglove.oneof(σ_i, \mathcal{G})`. The search space is of size $\binom{|E_{max}|}{|E|}$ or $2^{|E_{max}|}$ when using a fixed or variable size $|E|$ respectively.

3.1.2 Quantization

Pre-trained weights can also be quantized and thus effectively partitioned, with methods such as Huffman coding [19], randomized quantization [4], and hashing mechanisms [12]. As a strong baseline, [5] hardcodes RL policies using specific *Toeplitz* matrices (see: Fig. 2b) and found that such quantization patterns work well in continuous control.

For our **quantization** method, we assign to each edge (i, j) one color of many *colors* $c \in \mathcal{C} = \{1, \dots, |\mathcal{C}|\}$, denoting the partition group the edge is assigned to, which defines the value $w_{i,j} \leftarrow w^{(c)}$. This is shown pictorially in Figs. 2a and 2b. This can also programmatically be done by concatenating primitives `pyglove.oneof($e_{i,j}, \mathcal{C}$)` over all edges $e_{i,j} \in E_{max}$. The search space is of size $|\mathcal{C}|^{|E|}$.

3.2 Controller Comparisons

We first compare between the random, Policy Gradient (PG), and Reg-Evo controllers in Fig. 3 on the edge pruning task. While we clearly see that the random controller usually does poorly, we find that the PG and Reg-Evo controllers both perform well on various tasks, with one outperforming the other depending on the type of task. We further find that in most cases, the Reg-Evo controller converges much faster, although the PG controller may sometimes end up with a higher asymptotic performance. Intriguingly, PG produces generally higher variance between runs as well. This is intriguing, as there is no clear winner between PG and Reg-Evo, unlike in supervised learning (SL) where it is usually clear that the now widely adopted Reg-Evo outperforms PG [35].

On the topic of random search, we find our results somewhat consistent compared to NAS in supervised learning (SL) - random search in SL sampled from a reasonable search space can produce $\geq 80\%$ accuracy [34, 35] with the most gains from NAS ultimately be at the tail end; e.g. at the 95% accuracies, which is also shown to a lesser degree for easier RL environments such as Striker

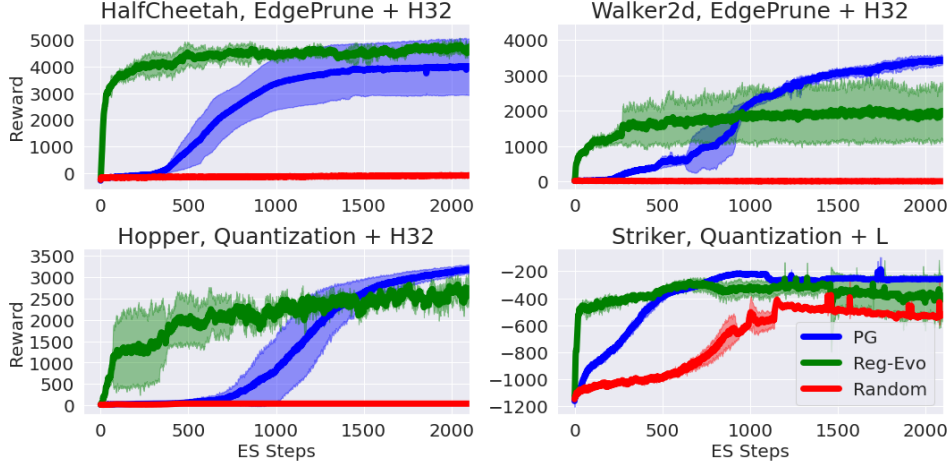


Figure 3: Comparisons across different environments when using different controllers, on the edge pruning and quantization tasks, when using a linear layer (L) or hidden layer of size 32 (H32).

(shown in Fig. 3) and Reacher (shown in Appendices B.2, B.3), although for the majority of RL environments, random search is unable to train at all.

3.3 Multiobjective Case

[47, 46] introduce the powerful notion of *multiobjective optimization*, where the controller may optimize multiple objectives towards a Pareto optimal solution [10]. We apply [46] and modify the controller’s objective to be a hybrid combination $f(\theta, m) \left(\frac{|E_m|}{|E_T|} \right)^\omega$ of both the total reward $f(\theta)$ and the compression ratio $\frac{|E_m|}{|E_T|}$ where $|E_m|$ is the number of edges in model m and $|E_T|$ is a target number, with the search space expressed as boolean mask mappings $(i, j) \rightarrow \{0, 1\}$ over all possible edges. For proof-of-concept, we follow the basic setting in [46] and set $\omega = -1$ if $\frac{|E_m|}{|E_T|} > 1$, while $\omega = 0$ otherwise, which strongly penalizes the controller if it proposes a model m whose edge number $|E_m|$ breaks the threshold $|E_T|$. However, as noted in [46], ω can be more finely tuned to allow $|E_T|$ to be a softer constraint and the hybrid objective to be smoother, if the user empirically knows the tradeoff between number of edges and reward.

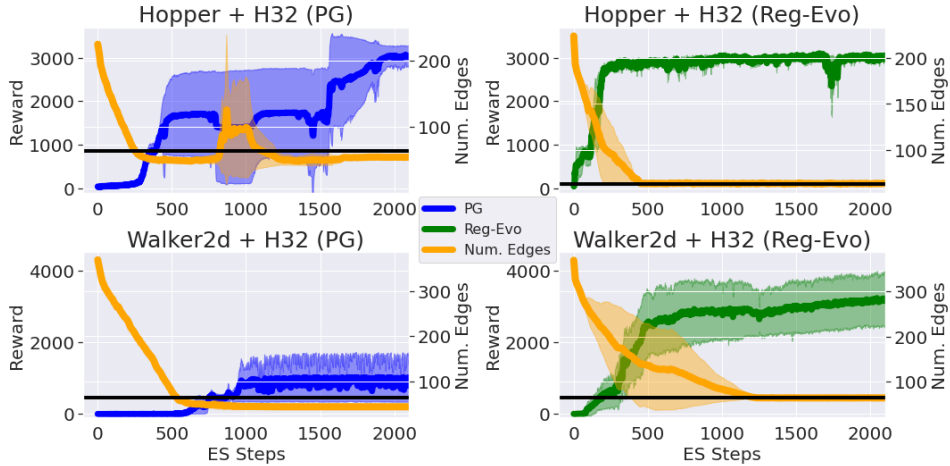


Figure 4: Environment reward plotted alongside the average number of edges used for proposed models. **Black** horizontal line corresponds to the target $|E_T| = 64$.

In Fig. 4, we see that the controller eventually reduces the number of edges below the target threshold set at $|E_T| = 64$, while still maintaining competitive training reward, demonstrating the versatility of the multiobjective approach in the RL setting.

3.4 Controller Sample Complexity

We further investigate the effect of the number of objective values per batch on the controller by randomly selecting only a subset of the objectives $f(m, \theta)$ for the controller p_ϕ to use, but maintain the original number of workers for updating θ_s via ES to maintain weight estimation quality to prevent confounding results. We found that this sample reduction can reduce the performance of both controllers for various tasks, especially the PG controller. Thus, we find the use of the already present ES workers highly crucial for the controller’s quality of architecture search in this setting.

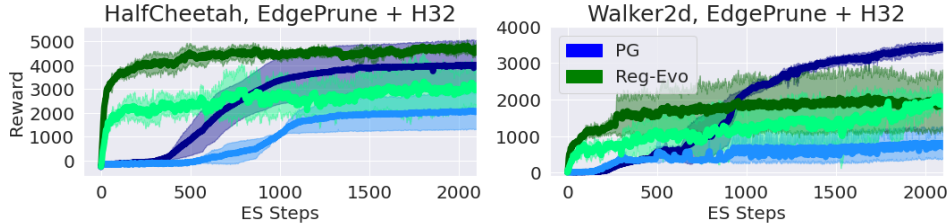


Figure 5: Regular ES-ENAS experiments with 150 full controller objective value usage plotted in darker colors. Experiments with lower controller sample usage (10 random samples, similar to the number of simultaneously training models in [46]) plotted in corresponding lighter colors.

3.5 Visualizing Convergence

We further graphically plot aggregate statistics over the controller samples to confirm ES-ENAS’s convergence. We choose the smallest environment, Swimmer, which conveniently works particularly well with *linear* policies [29], to reduce visual complexity and avoid permutation invariances. We also use a boolean mask space over all possible edges (search space size $|\mathcal{M}| = 2^{|\mathcal{S}| \times |\mathcal{A}|} = 2^{8 \times 2}$). We remarkably observe that *for all 3 independently seeded runs*, PG converges toward a specific “local maximum” architecture, demonstrated in Fig. 6 with the final architecture presented in Appendix A, which also depicts a similar case for Reg-Evo. This suggesting that there may be a few “natural architectures” optimal to the state representation.

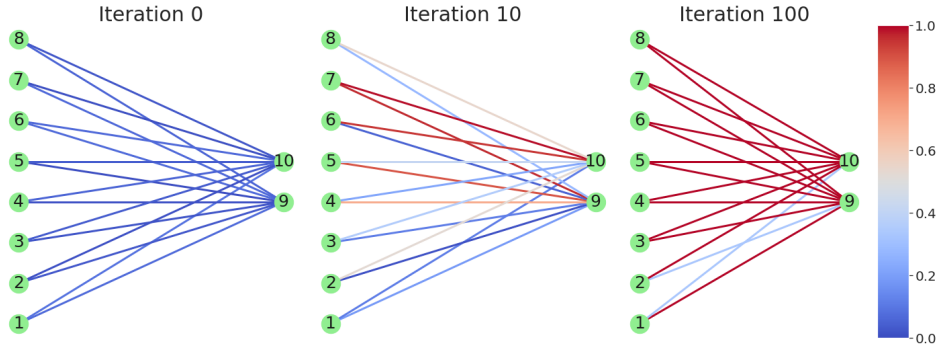


Figure 6: Edge pruning convergence over time, with samples aggregated over 3 seeds from PG runs on Swimmer. Each edge is colored according to a spectrum, with its color value equal to $2|p - \frac{1}{2}|$ where p is the edge frequency. We see that initially, each edge has uniform ($p = \frac{1}{2}$) probability of being selected, but as the controller trains, the samples converge toward a single pruning.

3.6 Full Results

Furthermore, we also include other search methods as baselines, including a DARTS-like [27] softmax *masking* method [26], where a trainable boolean matrix mask is drawn from a multinomial

distribution, and element-wise multiplied with the weights before a forward pass. We also include the results from using Toeplitz and Circulant (particular class of Toeplitz) matrices as weights from referenced works [5]. Specific details can be found in Appendices B.1 and C.2. The full set of numerical results over all of the mentioned methods can be found in Appendix B, which includes quantization (Appendix B.2), edge pruning (Appendix B.3), as well as plots for baseline methods (Fig. 9).

However, we present some of the more notable results in Table 1. Intriguingly, we found that appending the extra nonlinearity selection into the edge-pruning search space improved performance across HalfCheetah and Swimmer, but not across all environments (see Appendix B.3). However, lack of total improvement is consistent with the results found with WANNs [15], which also showed that trained WANNs’ performances matched with vanilla policies. From these two observations, we hypothesize that perhaps nonlinearity choice for simple MLP policies trained via ES are not quite so important to performance as other components, but more ablation studies must be conducted. Furthermore, for quantization policies, we see that hidden layer policies near-universally outperform linear policies, even when using the same number of distinct weights.

Env.	Dim.	(PG, Reg-Evo) Reward	Method
HalfCheetah	(17,6)	(2958, 3477) → (4258, 4894)	Quantization (L → H)
Hopper	(11,3)	(2097, 1650) → (3288, 2834)	Quantization (L → H)
HalfCheetah	(17,6)	(2372, 4016) → (3028, 5436)	Edge Pruning (H) → (+ Nonlinearity Search)
Swimmer	(8,2)	(105, 343) → (247, 359)	Edge Pruning (H) → (+ Nonlinearity Search)

Table 1: Rewards for selected environments and methods, each result averaged over 3 seeds. Arrow denotes modification or addition (+).

Env.	Arch.	Reward	# weights	compression	# bits
Striker	Quantization	-247	23	95%	8198
	Edge Pruning	-130	64	93%	3072
	Masked	-967	25	95%	8262
	Toeplitz	-129	110	88%	4832
	Circulant	-120	82	90%	3936
	Unstructured	-117	1230	0%	40672
HalfCheetah	Quantization	4894	17	94%	6571
	Edge Pruning	4016	64	98%	3072
	Masked	4806	40	92%	8250
	Toeplitz	2525	103	85%	4608
	Circulant	1728	82	88%	3936
	Unstructured	3614	943	0%	31488
Hopper	Quantization	3220	11	92%	3960
	Edge Pruning	3349	64	84%	3072
	Masked	2196	17	91%	4726
	Toeplitz	2749	94	78%	4320
	Circulant	2680	82	80%	3936
	Unstructured	2691	574	0%	19680
Walker2d	Quantization	2026	17	94%	6571
	Edge Pruning	3813	64	90%	3072
	Masked	1781	19	94%	6635
	Toeplitz	1	103	85%	4608
	Circulant	3	82	88%	3936
	Unstructured	2230	943	0%	31488

Table 2: Comparison of the best policies from six distinct classes of RL networks: Quantization (ours), Edge Pruning (ours), Masked, Toeplitz, Circulant, and Unstructured networks trained with standard ES algorithm [38]. All results are for feedforward nets with one hidden layer. Top two performing networks for each environment are in **bold**.

In Table 2 we directly compare our methods with the masking approach discussed in Subsection C.5 and (in more detail in Appendix B.1), as well as other structured policies (Toeplitz from [5] and Circulant) and the unstructured baseline. In all cases we use the same hyper-parameters, and train until convergence for three random seeds. For masking, we report the best achieved reward with > 90% of the network pruned, making the final policy comparable in size to the quantization and edge-pruning networks.

For each class of policies, we compare the number of weight parameters used (“# of weight-params” field), since the compactification mechanism does not operate on bias vectors. We also record compression with respect to unstructured networks in terms of the total number of parameters including biases (“# compression” field).

This number determines the reduction of sampling complexity with respect to unstructured networks (which is a bottleneck of ES training), since generally for ES, the number of blackbox function $f(\theta)$ queries needed to optimize f is proportional to the length of θ , which is equal to the total number of weights and biases of a policy network π_θ [23, 45, 2].

Finally, for a working policy we report total number of bits required to encode it assuming that real values are stored in the float format. Note that for quantization and masking methods, these include bits required to encode a dictionary representing the partitioning.

4 Limitations and Societal Impacts

We note that the backbone of our method for weight updating is ES, which utilizes blackbox/zeroth-order optimization. Zeroth order optimizations tend to struggle on larger numbers of parameters (100K+) due to the higher dimensionality of the parameter space [1].

We also benchmarked our method on an arguably "artificial" setting involving edge pruning and quantization for networks which are already relatively small and fast. While small architectures are still important for highly constrained resource settings such as mobile robotics [14], the search space design choice was mainly made in order to provide a large and challenging search space (10^{68}), larger than most SL NAS spaces [53, 11], to better stress test our controller-based method.

With regards to potential negative societal consequences, generally speaking, NAS methods can sacrifice model interpretability in order to achieve higher rewards. For the field of RL specifically, this may warrant more attention in AI safety when used for real world robotic pipelines. However, for our specific work, due to the smaller overall size of the policy networks, our results might actually be more interpretable - for instance, edge pruning may lead to discovery and disuse of MDP state values which do not contribute to obtaining high rewards, thereby improving a practitioner's understanding of the problem. Furthermore, as with any NAS research, the initial phase of discovery and experimentation may contribute to carbon emissions due to the computational costs of extensive tuning. However, this is usually a means to an end, such as an efficient search algorithm, which this paper proposes with no extra hardware costs.

5 Conclusion & Future Work

We presented a scalable and flexible algorithm, ES-ENAS, for performing efficient neural architecture search for reinforcement learning policies by combining Evolutionary Strategies with a controller-based techniques, which are generally considered some of the most effective within the deep learning field. ES-ENAS is also compatible with the latest frameworks such as PyGlove [33], as well as the latest techniques for NAS (multiobjective optimization [47, 46] and Regularized Evolution [35]).

We believe that this work can be the start of a new line of thinking for NAS methods applied to RL. One highly impactful application may be designing convolutional cells for vision-based RL policies to improve generalization [7, 8, 42], similar to the search spaces found in standard SL applications [34, 47, 53]. One may use similar search spaces to design EfficientNet variants for vision-based RL as well, an extension of the multiobjective experiments found in this paper for dense layers. We hope that applying NAS techniques in RL may ultimately automate architecture design for policies, as well as change perspectives on designing human-made policies.

Furthermore, our work is not only restricted to RL, but is applicable to blackbox optimization as a whole. Our method utilizes joint optimization between large-scale continuous parameter spaces (using ES) alongside discrete and conditional parameter spaces, which are used in the vast majority of hyperparameter tuning systems [17].

6 Acknowledgements

The authors would like to thank David Ha, Yingjie Miao, Aleksandra Faust, Sagi Perel, Daniel Golovin, John D. Co-Reyes, and Vikas Sindhwani for valuable discussions.

References

- [1] A. Agarwal, O. Dekel, and L. Xiao. Optimal algorithms for online convex optimization with multi-point bandit feedback. In A. T. Kalai and M. Mohri, editors, *COLT 2010 - The 23rd Conference on Learning Theory, Haifa, Israel, June 27-29, 2010*, pages 28–40. Omnipress, 2010.
- [2] A. Agarwal, D. P. Foster, D. J. Hsu, S. M. Kakade, and A. Rakhlin. Stochastic convex optimization with bandit feedback. In *Advances in Neural Information Processing Systems 24: 25th Annual Conference on Neural Information Processing Systems 2011. Proceedings of a meeting held 12-14 December 2011, Granada, Spain*, pages 1035–1043, 2011.
- [3] Y. Chauvin. A back-propagation algorithm with optimal use of hidden units. In D. S. Touretzky, editor, *Advances in Neural Information Processing Systems 1*, pages 519–526, San Francisco, CA, USA, 1989. Morgan Kaufmann Publishers Inc.
- [4] W. Chen, J. Wilson, S. Tyree, K. Weinberger, and Y. Chen. Compressing neural networks with the hashing trick. In *International Conference on Machine Learning*, pages 2285–2294, 2015.
- [5] K. Choromanski, M. Rowland, V. Sindhvani, R. E. Turner, and A. Weller. Structured evolution with compact architectures for scalable policy optimization. In *Proceedings of the 35th International Conference on Machine Learning, ICML 2018, Stockholmsmässan, Stockholm, Sweden, July 10-15, 2018*, pages 969–977, 2018.
- [6] J. D. Co-Reyes, Y. Miao, D. Peng, E. Real, S. Levine, Q. V. Le, H. Lee, and A. Faust. Evolving reinforcement learning algorithms. *CoRR*, abs/2101.03958, 2021.
- [7] K. Cobbe, C. Hesse, J. Hilton, and J. Schulman. Leveraging procedural generation to benchmark reinforcement learning. In *Proceedings of the 37th International Conference on Machine Learning, ICML 2020, 13-18 July 2020, Virtual Event*, pages 2048–2056, 2020.
- [8] K. Cobbe, O. Klimov, C. Hesse, T. Kim, and J. Schulman. Quantifying generalization in reinforcement learning. In *Proceedings of the 36th International Conference on Machine Learning, ICML 2019, 9-15 June 2019, Long Beach, California, USA*, pages 1282–1289, 2019.
- [9] Y. L. Cun, J. S. Denker, and S. A. Solla. Optimal brain damage. In D. S. Touretzky, editor, *Advances in Neural Information Processing Systems 2*, San Francisco, CA, USA, 1990. Morgan Kaufmann Publishers Inc.
- [10] K. Deb. *Multi-Objective Optimization*. Springer US, 2005.
- [11] X. Dong and Y. Yang. Nas-bench-201: Extending the scope of reproducible neural architecture search. In *8th International Conference on Learning Representations, ICLR 2020, Addis Ababa, Ethiopia, April 26-30, 2020*. OpenReview.net, 2020.
- [12] E. Eban, Y. Movshovitz-Attias, H. Wu, M. Sandler, A. Poon, Y. Idelbayev, and M. Á. Carreira-Perpiñán. Structured multi-hashing for model compression. In *2020 IEEE/CVF Conference on Computer Vision and Pattern Recognition, CVPR 2020, Seattle, WA, USA, June 13-19, 2020*, pages 11900–11909, 2020.
- [13] J. Frankle and M. Carbin. The lottery ticket hypothesis: Finding sparse, trainable neural networks. In *7th International Conference on Learning Representations, ICLR 2019, New Orleans, LA, USA, May 6-9, 2019*. OpenReview.net, 2019.
- [14] D. W. Gage, editor. *Mobile Robots XVII, Philadelphia, PA, USA, October 25, 2004*, volume 5609 of *SPIE Proceedings*. SPIE, 2002.
- [15] A. Gaier and D. Ha. Weight agnostic neural networks. In *Advances in Neural Information Processing Systems 32: Annual Conference on Neural Information Processing Systems 2019, NeurIPS 2019, December 8-14, 2019, Vancouver, BC, Canada*, pages 5365–5379, 2019.
- [16] D. E. Goldberg and K. Deb. A comparative analysis of selection schemes used in genetic algorithms. In *Proceedings of the First Workshop on Foundations of Genetic Algorithms. Bloomington Campus, Indiana, USA, July 15-18 1990*, pages 69–93, 1990.
- [17] D. Golovin, B. Solnik, S. Moitra, G. Kochanski, J. Karro, and D. Sculley. Google vizier: A service for black-box optimization. In *Proceedings of the 23rd ACM SIGKDD International Conference on Knowledge Discovery and Data Mining, Halifax, NS, Canada, August 13 - 17, 2017*, pages 1487–1495, 2017.

- [18] A. N. Gomez, I. Zhang, K. Swersky, Y. Gal, and G. E. Hinton. Learning sparse networks using targeted dropout. *ArXiv*, abs/1905.13678, 2019.
- [19] S. Han, H. Mao, and W. J. Dally. Deep compression: Compressing deep neural network with pruning, trained quantization and Huffman coding. In *International Conference on Learning Representations*, 2016.
- [20] S. Han, J. Pool, J. Tran, and W. Dally. Learning both weights and connections for efficient neural network. In C. Cortes, N. D. Lawrence, D. D. Lee, M. Sugiyama, and R. Garnett, editors, *Advances in Neural Information Processing Systems 28*, pages 1135–1143. Curran Associates, Inc., 2015.
- [21] N. Hansen, S. D. Müller, and P. Koumoutsakos. Reducing the time complexity of the de-randomized evolution strategy with covariance matrix adaptation (cma-es). *Evol. Comput.*, 11(1):1–18, Mar. 2003.
- [22] V. Heidrich-Meisner and C. Igel. Neuroevolution strategies for episodic reinforcement learning. *J. Algorithms*, 64(4):152–168, 2009.
- [23] K. G. Jamieson, R. D. Nowak, and B. Recht. Query complexity of derivative-free optimization. In *Advances in Neural Information Processing Systems 25: 26th Annual Conference on Neural Information Processing Systems 2012. Proceedings of a meeting held December 3-6, 2012, Lake Tahoe, Nevada, United States*, pages 2681–2689, 2012.
- [24] O. Krause. Large-scale noise-resilient evolution-strategies. In *Proceedings of the Genetic and Evolutionary Computation Conference, GECCO '19*, page 682–690, New York, NY, USA, 2019. Association for Computing Machinery.
- [25] O. Krause, D. R. Arbonès, and C. Igel. CMA-ES with optimal covariance update and storage complexity. In D. D. Lee, M. Sugiyama, U. von Luxburg, I. Guyon, and R. Garnett, editors, *Advances in Neural Information Processing Systems 29: Annual Conference on Neural Information Processing Systems 2016, December 5-10, 2016, Barcelona, Spain*, pages 370–378, 2016.
- [26] K. Lenc, E. Elsen, T. Schaul, and K. Simonyan. Non-differentiable supervised learning with evolution strategies and hybrid methods. *arXiv*, abs/1906.03139, 2019.
- [27] H. Liu, K. Simonyan, and Y. Yang. DARTS: differentiable architecture search. In *7th International Conference on Learning Representations, ICLR 2019, New Orleans, LA, USA, May 6-9, 2019*, 2019.
- [28] C. Louizos, M. Welling, and D. P. Kingma. Learning sparse neural networks through 10 regularization. In *International Conference on Learning Representations*, 2018.
- [29] H. Mania, A. Guy, and B. Recht. Simple random search of static linear policies is competitive for reinforcement learning. In *Advances in Neural Information Processing Systems*, pages 1800–1809, 2018.
- [30] H. Mania, A. Guy, and B. Recht. Simple random search provides a competitive approach to reinforcement learning. *CoRR*, abs/1803.07055, 2018.
- [31] M. C. Mozer and P. Smolensky. Skeletonization: A technique for trimming the fat from a network via relevance assessment. In D. S. Touretzky, editor, *Advances in Neural Information Processing Systems 1*, pages 107–115, San Francisco, CA, USA, 1989. Morgan Kaufmann Publishers Inc.
- [32] S. Narang, G. Diamos, S. Sengupta, and E. Elsen. Exploring sparsity in recurrent neural networks. In *International Conference on Learning Representations*, 2017.
- [33] D. Peng, X. Dong, E. Real, M. Tan, Y. Lu, G. Bender, H. Liu, A. Kraft, C. Liang, and Q. Le. Pyglove: Symbolic programming for automated machine learning. In *Advances in Neural Information Processing Systems 33: Annual Conference on Neural Information Processing Systems 2020, NeurIPS 2020, December 6-12, 2020, virtual*, 2020.
- [34] H. Pham, M. Y. Guan, B. Zoph, Q. V. Le, and J. Dean. Efficient neural architecture search via parameter sharing. In *Proceedings of the 35th International Conference on Machine Learning, ICML 2018, Stockholmsmässan, Stockholm, Sweden, July 10-15, 2018*, pages 4092–4101, 2018.
- [35] E. Real, A. Aggarwal, Y. Huang, and Q. V. Le. Regularized evolution for image classifier architecture search. *CoRR*, abs/1802.01548, 2018.

- [36] E. Real, C. Liang, D. R. So, and Q. V. Le. Automl-zero: Evolving machine learning algorithms from scratch. *CoRR*, abs/2003.03384, 2020.
- [37] D. E. Rumelhart. Personal communication. *Princeton*, 1987.
- [38] T. Salimans, J. Ho, X. Chen, S. Sidor, and I. Sutskever. Evolution strategies as a scalable alternative to reinforcement learning. *arXiv*, abs/1703.03864, 2017.
- [39] J. Schulman, F. Wolski, P. Dhariwal, A. Radford, and O. Klimov. Proximal policy optimization algorithms. *arXiv preprint arXiv:1707.06347*, 2016-2018.
- [40] A. See, M.-T. Luong, and C. D. Manning. Compression of neural machine translation models via pruning. In *Proceedings of The 20th SIGNLL Conference on Computational Natural Language Learning*, Berlin, Germany, Aug. 2016. Association for Computational Linguistics.
- [41] D. R. So, Q. V. Le, and C. Liang. The evolved transformer. In *Proceedings of the 36th International Conference on Machine Learning, ICML 2019, 9-15 June 2019, Long Beach, California, USA*, pages 5877–5886, 2019.
- [42] X. Song, Y. Jiang, S. Tu, Y. Du, and B. Neyshabur. Observational overfitting in reinforcement learning. In *8th International Conference on Learning Representations, ICLR 2020, Addis Ababa, Ethiopia, April 26-30, 2020*, 2020.
- [43] K. O. Stanley, D. B. D’Ambrosio, and J. Gauci. A hypercube-based encoding for evolving large-scale neural networks. *Artif. Life*, 15(2):185–212, 2009.
- [44] K. O. Stanley and R. Miikkulainen. Evolving neural network through augmenting topologies. *Evolutionary Computation*, 10(2):99–127, 2002.
- [45] R. Storn and K. V. Price. Differential evolution - A simple and efficient heuristic for global optimization over continuous spaces. *J. Glob. Optim.*, 11(4):341–359, 1997.
- [46] M. Tan, B. Chen, R. Pang, V. Vasudevan, and Q. V. Le. Mnasnet: Platform-aware neural architecture search for mobile. *CoRR*, abs/1807.11626, 2018.
- [47] M. Tan and Q. V. Le. Efficientnet: Rethinking model scaling for convolutional neural networks. In *Proceedings of the 36th International Conference on Machine Learning, ICML 2019, 9-15 June 2019, Long Beach, California, USA*, pages 6105–6114, 2019.
- [48] E. Todorov, T. Erez, and Y. Tassa. Mujoco: A physics engine for model-based control. In *2012 IEEE/RSJ International Conference on Intelligent Robots and Systems, IROS 2012, Vilamoura, Algarve, Portugal, October 7-12, 2012*, pages 5026–5033, 2012.
- [49] K. Varelas, A. Auger, D. Brockhoff, N. Hansen, O. A. ElHara, Y. Semet, R. Kassab, and F. Barbareco. A comparative study of large-scale variants of CMA-ES. In A. Auger, C. M. Fonseca, N. Lourenço, P. Machado, L. Paquete, and L. D. Whitley, editors, *Parallel Problem Solving from Nature - PPSN XV - 15th International Conference, Coimbra, Portugal, September 8-12, 2018, Proceedings, Part I*, volume 11101 of *Lecture Notes in Computer Science*, pages 3–15. Springer, 2018.
- [50] O. Vinyals, M. Fortunato, and N. Jaitly. Pointer networks. In *Advances in Neural Information Processing Systems 28: Annual Conference on Neural Information Processing Systems 2015, December 7-12, 2015, Montreal, Quebec, Canada*, pages 2692–2700, 2015.
- [51] D. Wierstra, T. Schaul, T. Glasmachers, Y. Sun, J. Peters, and J. Schmidhuber. Natural evolution strategies. *Journal of Machine Learning Research*, 15:949–980, 2014.
- [52] R. J. Williams. Simple statistical gradient-following algorithms for connectionist reinforcement learning. *Machine Learning*, 8:229–256, 1992.
- [53] C. Ying, A. Klein, E. Christiansen, E. Real, K. Murphy, and F. Hutter. Nas-bench-101: Towards reproducible neural architecture search. In *Proceedings of the 36th International Conference on Machine Learning, ICML 2019, 9-15 June 2019, Long Beach, California, USA*, pages 7105–7114, 2019.
- [54] B. Zoph and Q. V. Le. Neural architecture search with reinforcement learning. In *5th International Conference on Learning Representations, ICLR 2017, Toulon, France, April 24-26, 2017, Conference Track Proceedings*, 2017.

Appendix

A Network Visualizations

A.1 Quantization

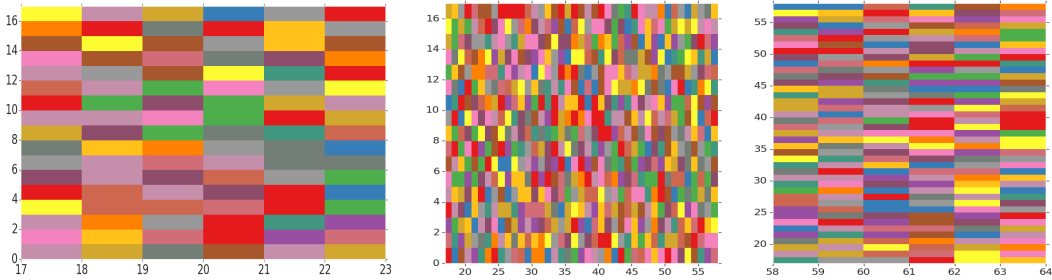


Figure 7: (a): Partitioning of edges into distinct weight classes obtained for the linear policy for HalfCheetah environment from OpenAI Gym. (b): Partitioning of edges for a policy with one hidden layer encoded by two matrices. State and action dimensionalities are: $s = 17$ and $a = 6$ respectively and hidden layer for the architecture from (b) is of size 41. Thus the size of the matrices are: 17×6 for the linear policy from (a) and: 17×41 , 41×6 for the nonlinear one from (b).

A.2 Edge Pruning

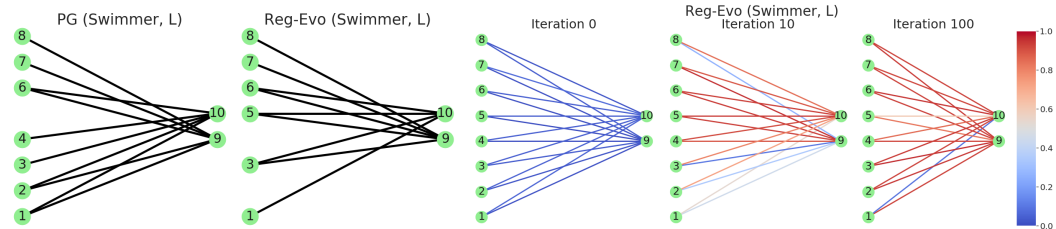


Figure 8: (Left) Final architectures that PG and Reg-Evo converged to on Swimmer with a linear (L) policy, as specified in Subsection 3.5. Note that the controller does not select all edges even if it is allowed in the boolean search space, but also *ignores some state values*. (Right): Convergence result for Reg-Evo, similar to Fig. 6 in Subsection 3.5.

B Extended Experimental Results

As standard in RL, we take the mean and standard deviation of the final rewards across 3 seeds for every setting. “L”, “H” and “H, H” stand for: linear policy, policy with one hidden layer, and policy with two such hidden layers respectively.

B.1 Baseline Method Comparisons

In terms of the masking baseline, while [26] fixes the sparsity of the mask, we instead initialize the sparsity at 50% and increasingly reward smaller networks (measured by the size of the mask $|m|$) during optimization to show the effect of pruning. Using this approach on several Open AI Gym tasks, we demonstrate that masking mechanism is capable of producing compact effective policies up to a high level of pruning. At the same time, we show significant decrease of performance at the 80-90% compression level, quantifying accurately its limits for RL tasks (see: Fig. 9).

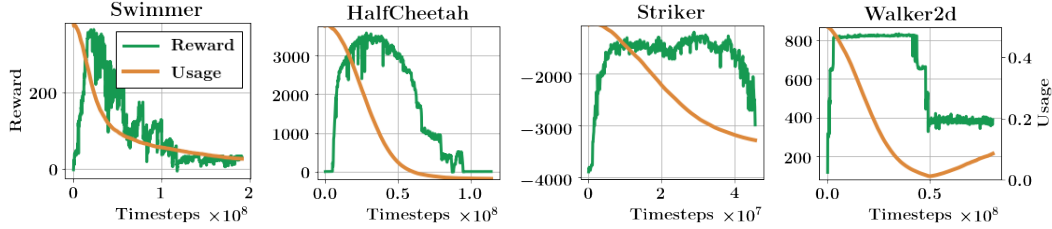


Figure 9: The results from training both a mask m and weights θ of a neural network with two hidden layers. ‘Usage’ stands for number of edges used after filtering defined by the mask. At the beginning, the mask is initialized such that $|m|$ is equal to 50% of the total number of parameters in the network.

B.2 Quantization

Env.	Dim.	Arch.	Partitions	(PG, Reg-Evo, RS) Reward
Swimmer	(8,2)	L	8	(366 ± 0, 296 ± 31, 5 ± 1)
Reacher	(11,2)	L	11	(−10 ± 4, −157 ± 62, −135 ± 10)
Hopper	(11,3)	L	11	(2097 ± 788, 1650 ± 320, 16 ± 0)
HalfCheetah	(17,6)	L	17	(2958 ± 73, 3477 ± 964, 129 ± 183)
Walker2d	(17,6)	L	17	(326 ± 86, 2079 ± 1085, 8 ± 0)
Pusher	(23,7)	L	23	(−68 ± 2, −198 ± 76, −503 ± 4)
Striker	(23,7)	L	23	(−247 ± 11, −376 ± 149, −590 ± 18)
Thrower	(23,7)	L	23	(−819 ± 8, −1555 ± 427, −12490 ± 708)

Env.	Dim.	Arch.	Partitions	(PG, Reg-Evo, RS) Reward
Swimmer	(8,2)	H	8	(361 ± 4, 362 ± 1, 15 ± 0)
Reacher	(11,2)	H	11	(−6 ± 0, −23 ± 11, −157 ± 2)
Hopper	(11,3)	H	11	(3288 ± 119, 2834 ± 75, 95 ± 2)
HalfCheetah	(17,6)	H	17	(4258 ± 1034, 4894 ± 110, −41 ± 5)
Walker2d	(17,6)	H	17	(1684 ± 1008, 2026 ± 46, −5 ± 1)
Pusher	(23,7)	H	23	(−225 ± 131, −350 ± 236, −1049 ± 40)
Striker	(23,7)	H	23	(−992 ± 2, −466 ± 238, −1009 ± 1)
Thrower	(23,7)	H	23	(−1873 ± 690, −818 ± 363, −12847 ± 172)

Table 3: Results via quantization across PG, Reg-Evo, and random search controllers. The number of partitions is always set to be $\max(|\mathcal{S}|, |\mathcal{A}|)$.

B.3 Edge Pruning

Env.	Dim.	Arch.	(PG, Reg-Evo, RS) Reward
Swimmer	(8,2)	H	(105 ± 116, 343 ± 2, 21 ± 1)
Reacher	(11,2)	H	(−16 ± 5, −52 ± 5, −160 ± 2)
Hopper	(11,3)	H	(3349 ± 206, 2589 ± 106, 66 ± 0)
HalfCheetah	(17,6)	H	(2372 ± 820, 4016 ± 726, −156 ± 22)
Walker2d	(17,6)	H	(3813 ± 128, 1847 ± 710, 0 ± 2)
Pusher	(23,7)	H	(−133 ± 31, −156 ± 17, −503 ± 15)
Striker	(23,7)	H	(−178 ± 54, −130 ± 16, −464 ± 13)
Thrower	(23,7)	H	(−532 ± 29, −1107 ± 158, −7797 ± 112)

Table 4: Results via quantization across PG, Reg-Evo, and random search controllers. The number of edges is always set to be 64 in total, or (32, 32) across the two weight matrices when using a single hidden layer.

Env.	Dim.	Arch.	(PG, Reg-Evo, RS) Reward
Swimmer	(8,2)	H	(247 ± 110, 359 ± 5, 11 ± 3)
Hopper	(11,3)	H	(2270 ± 1464, , 57 ± 7)
HalfCheetah	(17,6)	H	(3028 ± 469, 5436 ± 978, −268 ± 29)
Walker2d	(17,6)	H	(1057 ± 413, 2006 ± 248, 0 ± 1)

Table 5: Results using the same setup as Table 4, but allowing nonlinearity search.

C Exact Setup and Hyperparameters

C.1 Controller Setups

C.1.1 Regularized Evolution

We use uniform sampling, with the tournament size as \sqrt{n} where n is the number of workers (which is defaulted to 150; see: "ES Algorithm" subsection). This is also recommended in [35].

C.1.2 Policy Gradient

We use a gradient update batch size of 64 to the Pointer Network, while using PPO as the policy gradient algorithm, with its default (recommended) hyperparameters from [33].

C.2 Policy

By default, unless specified, we use Tanh non-linearities with 32 units for each hidden layer. We use the following default hyperparameters for the following search spaces:

C.2.1 Quantization

The number of partitions (or "colors") is set to $\max(|\mathcal{S}|, |\mathcal{A}|)$. This is both in order to ensure a linear number of trainable parameters compared to the quadratic number for unstructured networks, as well as allow sufficient parameterization to deal with the entire state/action values.

C.2.2 Edge Pruning

We collect all possible edges from a normal neural network into a pool E_{max} and set $|E| = 64$ as the number of distinct choices, passed to the `pygLove.manyof`. Similar to quantization, this choice is based on the value $\max(|\mathcal{S}|, H)$ or $\max(|\mathcal{A}|, H)$, where $H = 32$ is the number of hidden units, which is linear in proportion to respectively, the maximum number of weights $|\mathcal{S}| \cdot H$ or $|\mathcal{A}| \cdot H$. Since a hidden layer neural network has two weight matrices due to the hidden layer connecting to both the state and actions, we thus have ideally a maximum of $32 + 32 = 64$ edges.

C.2.3 Nonlinearity Search

We use the same nonlinearity choices found in [15]. These are: {Tanh, ReLU, Exp, Identity, Sin, Sigmoid, Absolute Value, Cosine, Square, Reciprocal, Step Function.}

C.3 Environment

For all environments, we set the horizon $T = 1000$. We also use the reward without alive bonuses for weight training as commonly used [29] to avoid local maximum behaviors (such as an agent simply standing still to collect a total of 1000 reward), but report the final score as the real reward with the alive bonus.

C.4 ES Algorithm

For all environments, we used reward normalization and state normalization implemented from [30]. We set smoothing parameter $\sigma = 0.1$ and step size $\eta = 0.01$. Unless specified, we use 150 workers, where 100 are used for perturbations in the antithetic case (and thus $100 / 2 = 50$ distinct perturbations are used) and 50 more are used for evaluation on the current parameter settings.

C.5 Baseline Details

We consider Unstructured, Toeplitz, Circulant and a masking mechanism [5, 26]. We introduce their details below. Notice that all baseline networks share the same general (1-hidden layer, Tanh nonlinearity) architecture from C.2. This implies that we only have two weight matrices $W_1 \in \mathbb{R}^{|\mathcal{S}| \times h}$, $W_2 \in \mathbb{R}^{h \times |\mathcal{A}|}$ and two bias vectors $b_1 \in \mathbb{R}^h$, $b_2 \in \mathbb{R}^{|\mathcal{A}|}$, where $|\mathcal{S}|, |\mathcal{A}|$ are dimensions of state/action spaces. These networks differ in how they parameterize the weight matrices. We have:

C.5.1 Unstructured.

A fully-connected layer with unstructured weight matrix $W \in \mathbb{R}^{a \times b}$ has a total of ab independent parameters.

C.5.2 Toeplitz.

A toeplitz weight matrix $W \in \mathbb{R}^{a \times b}$ has a total of $a+b-1$ independent parameters. This architecture has been shown to be effective in generating good performance on benchmark tasks yet compressing parameters [5].

C.5.3 Circulant.

A circulant weight matrix $W \in \mathbb{R}^{a \times b}$ is defined for square matrices $a = b$. We generalize this definition by considering a square matrix of size $n \times n$ where $n = \max\{a, b\}$ and then do a proper truncation. This produces n independent parameters.

C.5.4 Masking.

One additional technique for reducing the number of independent parameters in a weight matrix is to mask out redundant parameters [26]. This slightly differs from the other aforementioned architectures since these other architectures allow for parameter sharing while the masking mechanism carries out pruning. To be concrete, we consider a fully-connected matrix $W \in \mathbb{R}^{a \times b}$ with ab independent parameters. We also setup another mask weight $\Gamma \in \mathbb{R}^{a \times b}$. Then the mask is generated via

$$\Gamma' = \text{softmax}(\Gamma/\alpha)$$

where softmax is applied elementwise and α is a constant. We set $\alpha = 0.01$ so that the softmax is effectively a thresholding function which outputs near binary masks. We then treat the entire concatenated parameter $\theta = [W, \Gamma]$ as trainable parameters and optimize both using ES methods. Note that this softmax method can also be seen as an instance of the continuous relaxation method from DARTS [27]. At convergence, the effective number of parameter is $ab \cdot \lambda$ where λ is the proportion of Γ' components that are non-zero. During optimization, we implement a simple heuristics

that encourage sparse network: while maximizing the true environment return $f(\theta) = \sum_{t=1}^T r_t$, we also maximize the ratio $1 - \lambda$ of mask entries that are zero. The ultimate ES objective is: $f'(\theta) = \beta \cdot f(\theta) + (1 - \beta) \cdot (1 - \lambda)$, where $\beta \in [0, 1]$ is a combination coefficient which we anneal as training progresses. We also properly normalize $f(\theta)$ and $(1 - \lambda)$ before the linear combination to ensure that the procedure is not sensitive to reward scaling.